Transient Overexpression of TGF-β1 Induces Epithelial Mesenchymal Transition in the Rodent Peritoneum

Peter J. Margetts,* Philippe Bonniaud,† Limin Liu,* Catherine M. Hoff,‡ Clifford J. Holmes,‡ Judith A. West-Mays,† and Margaret M. Kelly†

**Division of Nephrology and †Department of Pathology and Molecular Medicine, McMaster University, Hamilton, Ontario, Canada; and ‡Renal Division Scientific Affairs, Baxter Healthcare Corporation, McGaw Park, Illinois*

Epithelial mesenchymal transition (EMT), a process involved in many growth and repair functions, has been identified in the peritoneal tissues of patients who undergo peritoneal dialysis. The sequence of changes in gene regulation and cellular events associated with EMT after TGF-β1–induced peritoneal fibrosis is reported. Sprague-Dawley rats received an intraperitoneal injection of an adenovirus vector that transfers active TGF-β1 (AdTGF-β1) or control adenovirus, AdDL. Animals were killed 0 to 21 days after infection. Peritoneal effluent and tissue were analyzed for markers of EMT. In the animals that were treated with AdTGF-β1, an increase in expression of genes associated with EMT and fibrosis, such as type I collagen A2, α-smooth muscle actin, and the zinc finger regulatory protein Snail, was identified. Transition of mesothelial cells 4 to 7 d after infection, with appearance of epithelial cells in the submesothelial zone 7 to 14 d after exposure to AdTGF-β1, was demonstrated. This phase was associated with disruption of the basement membrane and increased expression of matrix metalloproteinase 2. By 14 to 21 d after infection, there was evidence of restoration of normal submesothelial architecture. These findings suggest that EMT occurs *in vivo* after TGF-β1 overexpression in the peritoneum. Cellular changes and gene regulation associated with EMT are evident throughout the fibrogenic process and are not limited to early time points. This further supports the central role of TGF-β1 in peritoneal fibrosis and provides an important model to study the sequence of events involved in TGF-β1–induced EMT.

J Am Soc Nephrol 16: 425-436, 2005. doi: 10.1681/ASN.2004060436

Epithelial mesenchymal transition (EMT) is involved in a variety of normal physiologic processes, including gastrulation, heart formation, and palate closure during embryogenesis (1,2), as well as pathologic processes such as metastatic potential in malignancy (3,4), and renal fibrogenesis (5,6). Moreover, EMT has been identified in peritoneal mesothelial cells exposed to TGF-β1 (7), and recently, *in vivo* evidence was found for EMT in patients who are on peritoneal dialysis (PD) (8). The steps in EMT include a loss of cell–cell and cell–matrix interaction through downregulation of E-cadherin and β-catenin (1,9), migration, basement membrane degradation through matrix metalloproteinase-2 (MMP-2) (10), and cytoskeletal rearrangement with expression of α-smooth muscle actin (α-SMA) (11), all events that are a normal part of tissue repair but could also contribute to chronic fibrosis.

In fibrotic disorders, the myofibroblast has been identified as one of the major cellular components involved in collagen deposition, and its presence correlates with progression of the disease (12). The origin of the myofibroblast has not been clearly defined, but recent studies in bone marrow chimeric mice confirm the role of mesenchymal transition over recruitment of circulating cell populations as the precursors of interstitial myofibroblasts (13).

Peritoneal fibrosis is a ubiquitous process in patients who are on PD (14). The importance of mild peritoneal fibrosis is uncertain, but we have previously shown an association between fibrogenesis and angiogenesis in the peritoneum after exposure to TGF-β1 (15). Increased vascular surface area of the peritoneum has been hypothesized to increase solute transport and lead to ultrafiltration dysfunction in PD patients (16). Encapsulating peritoneal sclerosis is a rare but devastating fibrotic complication seen in a variety of settings including PD (17). Therefore, peritoneal fibrosis is a potential severe limitation for patients who are reliant on PD for renal replacement therapy.

In this study, we induced peritoneal fibrosis using adenovirus-mediated gene transfer of active TGF-β1 to the rat peritoneum and analyzed peritoneal tissue at early (days 1 to 4 after infection) and later (days 7, 14, and 21) time points to identify markers of EMT. We observed an early increased expression of the EMT-related regulatory protein Snail along with increased expression of α-SMA, MMP-2, and type I collagen gene expression. In tissue sections, using dual-labeled immunofluorescence, we identified an early increase in dual-staining α-SMA and cytokeratin-positive cells in the mesothelial cell layer, with an increase in α-SMA–positive cells immediately beneath the mesothelial cells. At later time points, we could identify cells with both epithelial and myofibroblast characteristics within

Received June 3, 2004. Accepted October 22, 2004.

Published online ahead of print. Publication date available at www.jasn.org.

Address correspondence to: Dr. Peter J. Margetts, Department of Medicine, McMaster University, Division of Nephrology, Street Joseph's Hospital, 50 Charlton Avenue E, Hamilton, Ontario, Canada, L8P 4A6. Phone: 905-522-1155; Fax: 905-521-6068; E-mail: margetts@mcmaster.ca

Copyright © 2005 by the American Society of Nephrology

ISSN: 1046-6673/1602-0425

the submesothelial tissue. There was evidence of migration of cells through a disrupted basement membrane structure. It is interesting that, *in vivo*, we found increased gene and protein expression of E-cadherin, which is opposite to what we and others have found in *in vitro* experiments.

This study supports the role of EMT in peritoneal fibrosis and confirms the role of TGF-β1 in this process. *In vivo* models of EMT are not readily available, and this simple model allows the identification of the temporal sequence of TGF-β1–induced EMT and will allow further research into this important physiologic event.

Materials and Methods

Adenovirus

The construction of the adenovirus vector AdTGF-β1 has been previously described (18). AdTGF-β1 was created with TGF-β1 cDNA mutated at residues 223 and 225 so that the transgene product does not bind to the latency-associated protein and therefore is biologically active. To control for adenovirus effects, a null adenovirus (AdDL) was used (19). Adenovirus preparations were purified by CsCl gradient centrifugation and PD-10 Sephadex chromatography (Amersham Pharmacia, Baie d'Urfe, PQ, Canada) and plaque titered on 293 cells as described previously (20).

Animals. All animal studies were carried out according to the Canadian Council on Animal Care Guidelines. Two groups of female Sprague-Dawley rats (Harlan, Indianapolis, IN) that weighed 200 to 250 g received an intraperitoneal injection of AdTGF-β1 ($n = 46$) or control adenovirus ($n = 21$). All were administered adenovirus at a dose of 1.5×10^9 plaque-forming units (pfu)/ml diluted to 100 μl in PBS on day 0. No attempt was made to block the anti-adenoviral inflammatory response. This dose was similar to that used in previous experiments (15). Animals that were infected with AdTGF-β1 were killed on days 1 to 4, 7, 14, or 21 after adenovirus administration. AdDL-treated animals were killed on days 1 to 4, or 21. At early time points (days 1 to 3), four animals per group were killed. At later time points (days 4 to 21), 6 to 10 animals were killed. A third group of naïve rats ($n = 6$) were killed for control. Before the rats were killed, 0.09 ml/g 2.5% Dianeal (Baxter Healthcare, McGaw Park, IL) was administered intraperitoneally. Four hours later, the animal was killed, the peritoneum was opened, and the entire fluid content was removed. The entire anterior abdominal wall was removed after skin and subcutaneous tissues were removed. The lower or caudal portion of this tissue was stored in 4% neutral-buffered formalin, and the upper or rostral portion was taken for RNA extraction. Omental tissue was taken and frozen in liquid nitrogen.

Cell Culture

Primary mesothelial cells were isolated from rat peritoneum as described previously (15). Briefly, the anterior abdominal wall from naïve rats was isolated, washed with PBS, and covered with 10% trypsin (Invitrogen, Burlington, ON, Canada) for 45 min. The trypsin was then removed and centrifuged, and the cell pellet was resuspended in F12 medium supplemented with 10% FCS, 1% penicillin/streptomycin, and 0.08% Fungizone (Invitrogen). Cells were grown to confluence in six-well plates and then rested for 12 h in medium with 1% FCS. Cells then were exposed to varying concentrations of recombinant TGF-β1 (R&D Systems,

Table 1. Quantitative PCR probe and primer pairs[a]

Species	Forward Primer	Reverse Primer	Probe
Snail	GCCGGAAGCCCAACTATAGC	AGGGCTCGTGGAAGGTGAA	AGCTGCAGGACGCGTGTGTGGA
MMP-2	TGAGCTCCCGGAAAAGATTG	CATTCCCTGCGAAGAACACA	TGCCGTGTACGAGGCCCCACA
COL1A2	CCCAGCCAAGAATGCATACA	TCAAACTGGCTGCCACCAT	TGCCCAGGCCAACAAGCATGTC
E-cadherin	GGCCCAGGAGCTGACAAAC	CCAGAGGCTGCGTCACTTTC	CATCATTGAGAGGGAGACAGGCTGGC
α-SMA	CACGGCATCATCACCAACTG	CCACGCGAAGCTCGTTATAGA	CGACATGGAAAAGATCTGGCACCACTC
18S	GCCGCTAGAGG-TGAAATTCTTG	CATTCTTGGCAAATGCTTTCG	ACCGGCGCAAGACGGACCAGT

[a]MMP-2, matrix metalloproteinase-2; α-SMA, α-smooth muscle actin.

Table 2. Inflammatory response after adenovirus administration[a]

Day	Control	AdTGF-β1					AdDL			
	0	1	2	3	4	7	1	2	3	4
TNF-α (pg/ml)	58 ± 7	62 ± 8	61 ± 10	302 ± 417	65 ± 19	ND	52 ± 12	112 ± 103	524 ± 406	50 ± 4
Total cells (10^4/ml)	61 ± 6	42 ± 20	58 ± 21	535 ± 879	30 ± 27	73 ± 48	91 ± 42	661 ± 772	508 ± 401	74 ± 31
Neutrophils (10^4/ml)	2.3 ± 2.2	1.8 ± 1.8	7.6 ± 6.3	432 ± 740	0.1 ± 0.4	0.5 ± 0.8	3.7 ± 2.1	427 ± 603	341 ± 332	0.4 ± 0.7

[a]Inflammation, measured by peritoneal effluent TNF-α, cell count, and neutrophilia, was apparent on days 2 and 3 after infection with both AdTGF-β1 and AdDL. This response resolved by day 4 after infection. ND, no data.

Figure 1. Histology of the anterior abdominal wall. (A) Untreated animal (day 0). (B) Control adenovirus (AdDL)-treated animal, day 3. There is a mesothelial cell reaction (arrow) and increased interstitial cellularity. (C) AdTGF-β1 d 4 demonstrates mesothelial cell reaction, increased interstitial cellularity, submesothelial thickening, collagen deposition (closed arrow), and angiogenesis (open arrow). Magnification, ×100, Masson's trichrome.

Minneapolis, MN). Cell cultures had typical cobblestone appearance on phase contrast microscopy. Each culture condition was repeated in triplicate, and the entire experiment was repeated in duplicate.

Histology

Tissue samples from the lower portion of the anterior abdominal wall were fixed in 10% buffered formalin for 24 h. These samples then were processed and paraffin embedded, and sections were cut at 5 μm. Sections then were stained for Masson's trichrome or processed for immunohistochemistry using antibodies against α-SMA or laminin (Dako Corp., Carpinteria, CA) (15).

Dual staining with antibodies to α-SMA and cytokeratin (B&D Bioscience) was performed using fluorescently labeled antibodies. After antigen retrieval in boiling 10 mM citrate buffer (pH 6.0) for 45 min, sections were incubated with α-SMA antibody followed by a secondary rabbit anti-mouse antibody labeled with Texas Red (Molecular Probes, Eugene, OR). Sections then were stained with a FITC-labeled antibody to cytokeratin (Sigma Chemicals, Oakville, ON, Canada) and mounted with a DAPI nuclear stain (Vectashield, Vector Technologies). After the same antigen retrieval process, single staining with a FITC-labeled anti–E-cadherin antibody (B&D Bioscience) was also performed. These sections were viewed with a Leica DMR fluorescence microscope (Leica Microsystems, Wetzlar, Germany). Negative control sections were run in parallel with nonimmune mouse or rabbit serum for immunohistochemistry and immunofluorescence staining.

Anterior abdominal wall tissue was fixed in 2% glutaraldehyde in sodium cacodylate buffer (pH 7.4) for 24 h. The tissue then was rinsed in sodium cacodylate buffer, postfixed in 1% osmium tetroxide for 1 h, dehydrated in graded ethanol solutions, and embedded in Spurr's resin. Ultrathin sections (90 nm) were cut and placed on a 200-mesh thin bar copper grid and stained with uranyl acetate and lead citrate. The specimens were examined with a Philips CM10 transmission electron microscope.

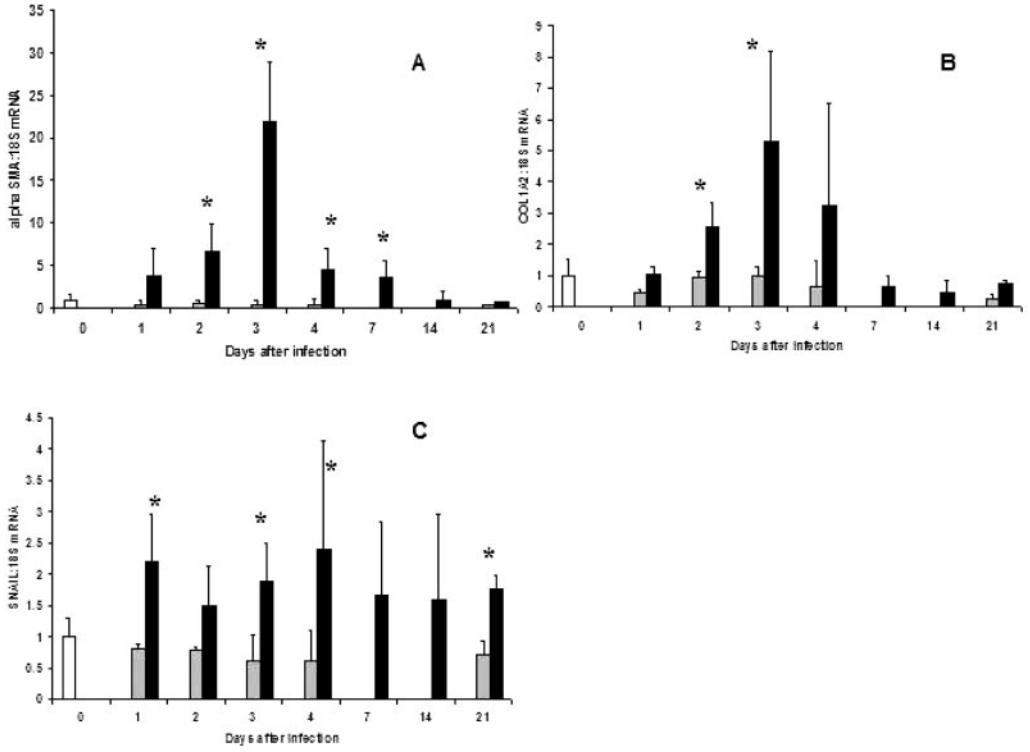

Figure 2. mRNA extracted from the anterior abdominal wall of untreated rats (□), AdTGF-β1–treated rats (■), or AdDL-treated animals (▨) and analyzed using quantitative real-time PCR for α-smooth muscle actin (α-SMA; A), type 1 collagen A2 (B), and Snail (C). Gene expression is normalized to 18S expression. Results demonstrate a strong upregulation of fibrosis-related gene expression (A and B). There is an associated increase in Snail expression (C). Snail is upregulated early after AdTGF-β1 infection and remains elevated until day 21 (C). Control adenovirus did not induce significant expression in any of these fibrosis or epithelial mesenchymal transition (EMT)-related genes. $^*P < 0.01$, AdTGF-β1 *versus* control.

Quantitative PCR

mRNA was extracted from the peritoneum of killed animals by immersing the parietal peritoneal surface in Trizol reagent (Invitrogen) for 20 min. Histologic analysis of tissues after Trizol exposure indicated that RNA was extracted predominantly from mesothelial and submesothelial tissue with little involvement of the submesothelial skeletal muscle (data not shown). For mesothelial cell culture experiments, confluent cells in six-well plates, exposed to recombinant TGF-β1, were lysed in Trizol. RNA was extracted from Trizol according to the manufacturer's instruction. RNA integrity and concentration were determined with an Agilent 2100 bioanalyzer (Agilent Technologies, Missisauga, ON, Canada). RNA (1 μg) then was DNAse treated and reverse-transcribed using a standard protocol (Invitrogen). Quantitative real-time PCR for Snail, MMP-2 type 1 collagen A2 (COL1A2), E-cadherin, and α-SMA was carried out using an ABI Prism 7700 Sequence Detector (Applied Biosystems, Foster City, CA). Pooled mRNA from control animals was used to create a standard curve for comparative quantification. The correlation coefficient for the standard curves all were >0.90. Samples were run in duplicate and multiplexed with glyceraldehyde-3-phosphate dehydrogenase probe and primer (Applied Biosystems). Negative control samples (no template or no reverse transcriptase) were run concurrently. Primers (Mobix, Hamilton, ON, Canada) and probes (Applied Biosystems) are shown in Table 1. Target gene probes were labeled with FAM reporter, and housekeeping gene probe was labeled with VIC. Similar results were observed referenced to either glyceraldehyde-3-phosphate dehydrogenase or 18S. Results are reported as relative to 18S RNA.

Peritoneal Fluid Analysis

After a 4-h dwell, peritoneal fluid was taken and the inflammatory response to adenovirus was assessed. A differential cell count was performed, and peritoneal fluid was analyzed for rat TNF-α using commercially available ELISA kits (R&D Systems).

MMP-2 content in the peritoneal effluent was studied using zymography. Equal volumes of peritoneal fluid were separated using 12% SDS-PAGE with the addition of gelatin (1 mg/ml; Sigma Chemicals). The gel was incubated in a solution of 2.5% Triton X-100 (Sigma Chemicals) for 30 min, incubated overnight at 37°C in an activating buffer (50 mM Tris-HCl [pH 8], 10 mM $CaCl_2$, 150 nm $ZnSO_4$, and 150 mM NaCl), stained with Coomassie Brilliant Blue R250 (Bio-Rad, Mississauga, ON, Canada) for 30 min and destained in a solution of 7.5% acetic acid and 5% methanol. MMP-2 and -9 standards were run concurrently (Chemicon, Temecula, CA).

Western Blot

Protein was extracted from frozen omental peritoneal tissue by homogenization in a standard lysis buffer with addition of proteinase inhibitors (sodium orthovanadate, phenylmethylsulfonyl fluoride, leupeptin, and aprotinin; all from BioShop, Burlington, ON, Canada), Twenty micrograms was electrophoresed on an 12% SDS-PAGE gel, transferred to a nylon membrane, and probed with an antibody to E-cadherin (BD Biosciences, Mississauga, ON, Canada). E-cadherin protein was visualized with enhanced chemiluminescences detection (Amersham Biotech, Piscataway, NJ).

Statistical Analyses

Data are presented as mean ± SD. Comparison between groups was made by independent *t* test. $P < 0.05$ was considered to be significant, and all tests were two-tailed.

Results

Adenovirus Infection Induces a Transient Peritonitis

To evaluate the potentially confounding effect of inflammatory response to adenovirus, we analyzed peritoneal effluent and tissue sections for evidence of inflammatory response. Intraperitoneal administration of both control adenovirus and AdTGF-β1 induced a transient, mild peritonitis characterized by an approximately 10-fold increase in peritoneal effluent concentrations of TNF-α 3 d after adenoviral infection (Table 2). There was an associated increase in peritoneal effluent cellularity (Table 2) that was predominantly neutrophilic. These measures of peritoneal inflammation all resolved back to baseline by day 4 after adenoviral infection.

Histologically, there was a mesothelial cell reaction with rounding of the normally flattened mesothelial cells and increased interstitial cellularity induced by AdDL compared to untreated animals (Figure 1A). This was most prominent 2 d after infection (Figure 1B). This transient inflammatory response may have played a role in the subsequently observed EMT. However, EMT was not observed in control animals, so we conclude that TGF-β1 was also essential for EMT in this model.

AdTGF-β1 Induces Peritoneal Fibrosis

As we have previously demonstrated (15), AdTGF-β1 induces a potent peritoneal fibrosis. In the present study, we confirmed that there was an induction of fibrosis as early as 4 d after exposure to TGF-β1, by both histologic evaluation (Figure 1C) and quantitative real-time PCR for COL1A2 (Figure 2B). Gene expression of COL1A2 and α-SMA (Figure 2A) was maximal at day 4 and declined back to baseline by day 21.

Gene Regulation after TGF-β1–Induced EMT in Peritoneal Tissues

Genes involved in EMT were regulated in peritoneal tissues shortly after infection with AdTGF-β1. There was a significant increase in mRNA and protein expression of α-SMA (Figures 2A and 3), as well as an increase in Snail gene expression (Figure 2C). Changes in expression of this EMT-related gene persisted to day 21.

Cellular Changes Associated with EMT in Peritoneal Tissues

Over the first 4 d of observation, there was a progressive increase in the expression of α-SMA in the submesothelial tissue of the peritoneal membrane (Figure 3). Four days after infection with AdTGF-β1, immunofluorescence demonstrated the appearance of dual-labeled cytokeratin and α-SMA–positive cells within the mesothelial cell layer (Figure 4, A through C). At days 7 and 14, cytokeratin-positive epithelial cells were found within the submesothelial tissue and were intermingled with α-SMA–positive myofibroblasts (Figure 4, D through I). Dual-labeled cytokeratin and α-SMA–positive cells were also

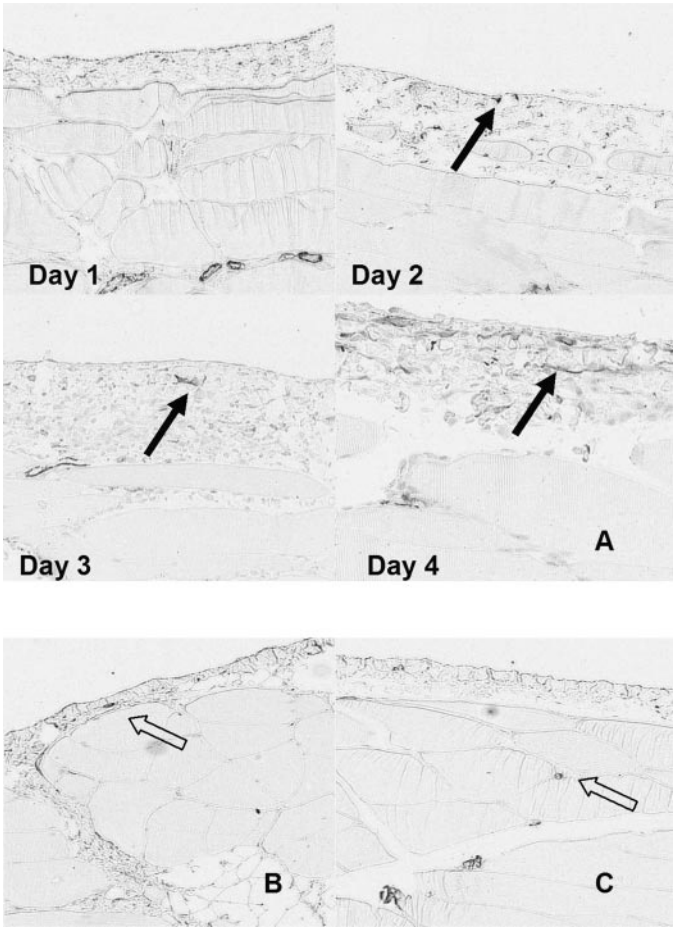

Figure 3. α-SMA expression in submesothelial tissue. There was a daily increase in submesothelial α-SMA–positive cells after AdTGF-β1 infection (A, closed arrows). Aside from perivascular cells (open arrows), there was no α-SMA expression in untreated control animals (B) or AdDL-treated animals (C). Magnification, ×100.

observed at day 7 within the interstitium but were not seen at day 14 (Figure 4, D through I). Electron microscopy revealed the presence of fibroblasts migrating through a basement membrane structure by day 4 (Figure 5B). The presence of myofibroblasts was confirmed by ultrastructural examination of peritoneal tissue 7 d after infection with AdTGF-β1 (Figure 5, C and E). There was direct evidence at days 4 and 7 on immunofluorescence (Figure 4, A through F) of EMT with cells staining for both cytokeratin and α-SMA. This was also suggested by electron microscopy, with mesothelial cells showing the development of probable intracellular microfilaments (Figure 5D). There was evidence of loss of an intact mesothelial cell layer in dual-labeled sections (Figures 4, D through I, and 5C) 7 and 14 d after infection with AdTGF-β1. Fluorescence and ultrastructural studies suggested that migratory behavior, cellular transition, and loss or detachment of mesothelium were maximal at day 7 after AdTGF-β1 infection. By day 21, there was resolution of these changes suggestive of EMT with evidence of re-mesothelialization (Figure 4J). There was no induced expres-

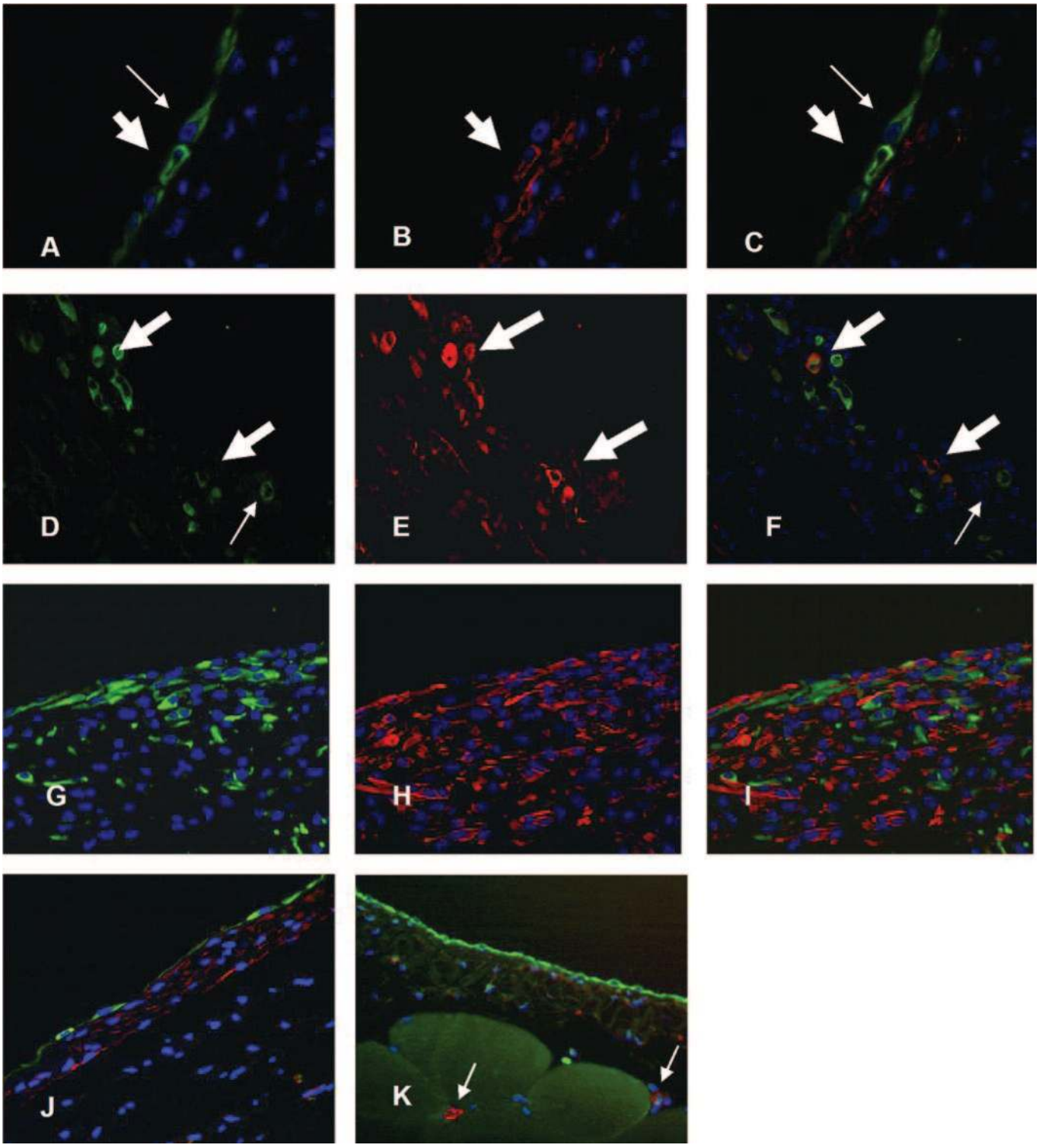

Figure 4. Immunofluorescence from anterior abdominal wall sections stained for cytokeratin (green) and α-SMA (red) with nuclear counterstain (blue, DAPI). (A through C) Four days after infection with AdTGF-β1 there is an increase in submesothelial α-SMA–positive myofibroblasts. The mesothelial cell layer demonstrates cytokeratin-positive cells (thin arrow) and dual-stained cytokeratin and α-SMA–positive cells (thick arrow). (D through F) At 7 d after infection with AdTGF-β1, epithelial cells (green, thin arrow) are present in the interstitium, and some of these cells stain for both cytokeratin and α-SMA (thick arrows). (G through I) Fourteen days after AdTGF-β1 infection, there is no evidence for dual-staining cells in the mesothelium; however, there are many intermingled single-staining cytokeratin or α-SMA–positive cells in the submesothelial zone. (J) Twenty-one days after AdTGF-β1 infection, there are remnant α-SMA–positive cells beneath a single mesothelial cell layer and no evidence of dual-stained cells. (K) AdDL-treated animal shows a single mesothelial cell layer with no submesothelial α-SMA staining aside from perivascular cells (thin arrows). Magnification, ×400 in A through C; ×200 in D through I; ×100 in J and K.

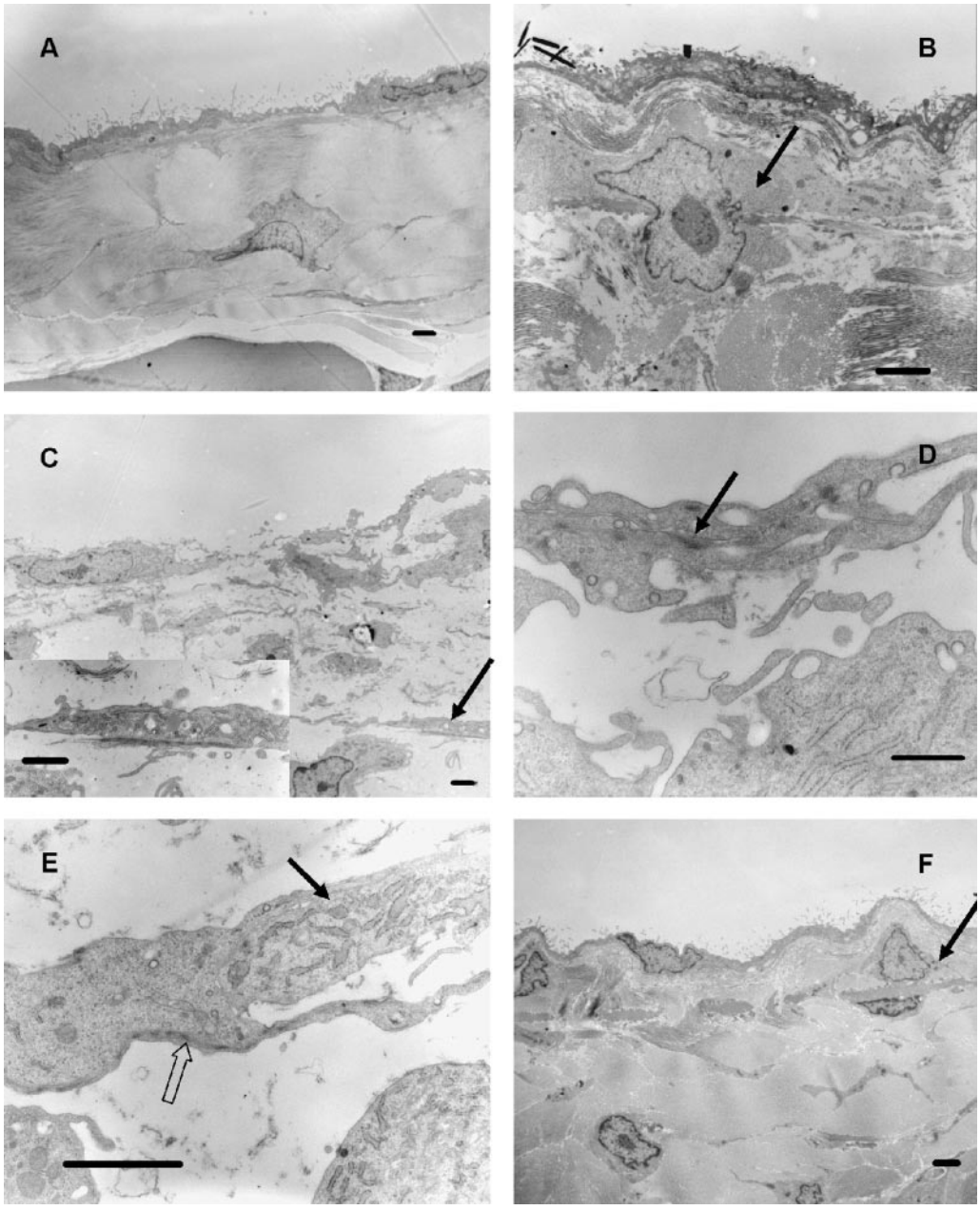

Figure 5. Electron micrographs of parietal peritoneum. (A) AdDL-treated animals show normal ciliated mesothelium, submesothelial basement membrane, interstitial matrix, and fibroblast lying over skeletal muscle. (B) Four days after infection with AdTGF-β1, a fibroblast is seen transiting through a basement membrane–like structure (arrow). (C) Seven days after infection with AdTGF-β1, there is extensive disruption of the submesothelial tissue with the appearance of typical myofibroblasts (arrow). Insert shows detail of intracytoplasmic fibrils. (D) Seven days after infection with AdTGF-β1, mesothelial cells seem activated, less adherent, and with filament structures (arrow) suggesting transition to myofibroblast phenotype. (E) Seven days after AdTGF-β1, a myofibroblast is demonstrated with extensive rough endoplasmic reticulum (closed arrow) and intracytoplasmic fibrils (open arrows). (F) Fourteen days after AdTGF-β1, the mesothelial layer is reestablished with submesothelial fibroblasts apparently involved in the creation of a new basement membrane structure (arrow). Bar = 2 μm.

sion of α-SMA or observed myofibroblasts in AdDL-treated animals (Figures 4K and 5A) or in untreated control animals.

Changes in Basement Membrane during TGF-β1–Induced EMT

We used laminin-stained sections and electron microscopy to evaluate changes in the submesothelial basement membrane. There was a basement membrane structure identified directly beneath the mesothelial cell layer in AdDL-treated animals (Figures 5A and 6A). Four days after AdTGF-β1, laminin expression was significantly increased, with the basement membrane structure now appearing several cells deep beneath the mesothelial layer (Figure 6B). By electron microscopy, fibroblasts can be observed moving through this basement membrane structure (Fig-

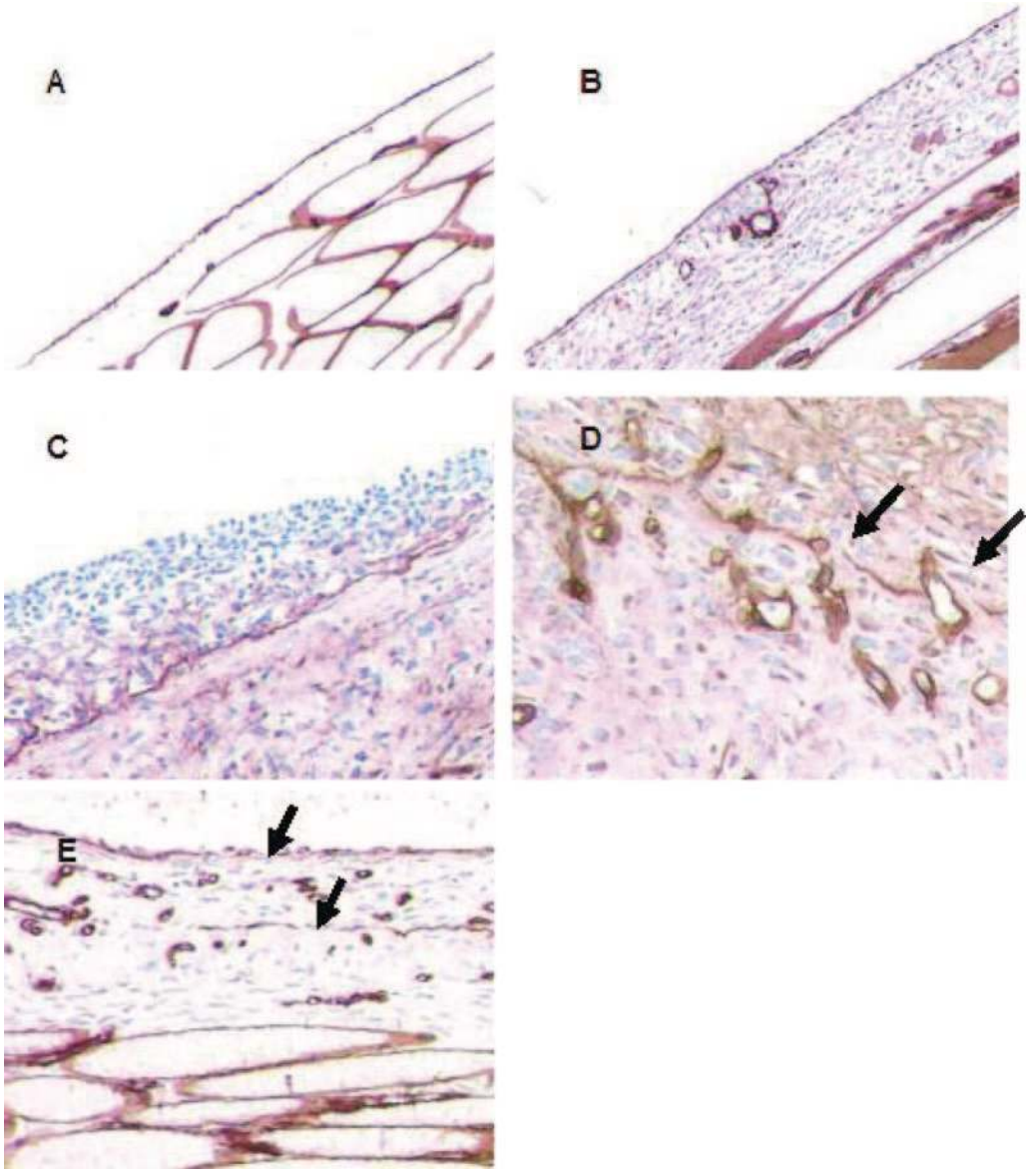

Figure 6. Laminin immunohistochemistry of submesothelial tissue demonstrates the sequence of basement membrane changes after overexpression of TGF-β1. (A) AdDL-treated animal shows a single, submesothelial basement membrane structure. (B) Four days after AdTGF-β1, the basement membrane remains intact with expansion of the submesothelial tissue and angiogenesis. (C) Seven days after AdTGF-β1, there is cellular proliferation both above and below the basement membrane with disruption of the basement membrane and transit of cells and blood vessels across the membrane (seen in D, arrows). (E) Day 14 after AdTGF-β1 shows a residual basement membrane structure 50 to 100 μm below the new mesothelial surface with creation of a secondary submesothelial basement membrane (arrows). Magnification, $\times$100 in A through C and E; $\times$200 in D.

ure 5B). By day 7, there was cellular expansion both above and below the basement membrane structure, loss of continuity, and transit of cells and blood vessels through this structure (Figure 6, C and D). By day 14, there was a new basement membrane formed beneath the re-epithelialized peritoneal surface, with traces of the original basement membrane identified 50 to 100 μm beneath the new peritoneal surface (Figure 6E). Ultrastructural studies of peritoneal samples 14 d after infection with AdTGF-β1 suggest that submesothelial fibroblasts are involved in the creation of the new basement membrane (Figure 5F). This progressive destruction of the original basement membrane histologically occurs between days 4 and 14 after AdTGF-β1 infection and corresponds to the increased gene and protein expression of MMP-2 (Figure 7).

TGF-β1 Induces Increased Expression of E-Cadherin

Contrary to the evidence from *in vitro* experiments, we found that animals that were exposed to increased intraperitoneal expression of TGF-β1 demonstrated increased protein expression of E-cadherin with increase in gene expression 2 to 7 d after adenoviral infection (Figure 8). Protein and cellular localization (Figure 8, B and C) suggests an increase in both

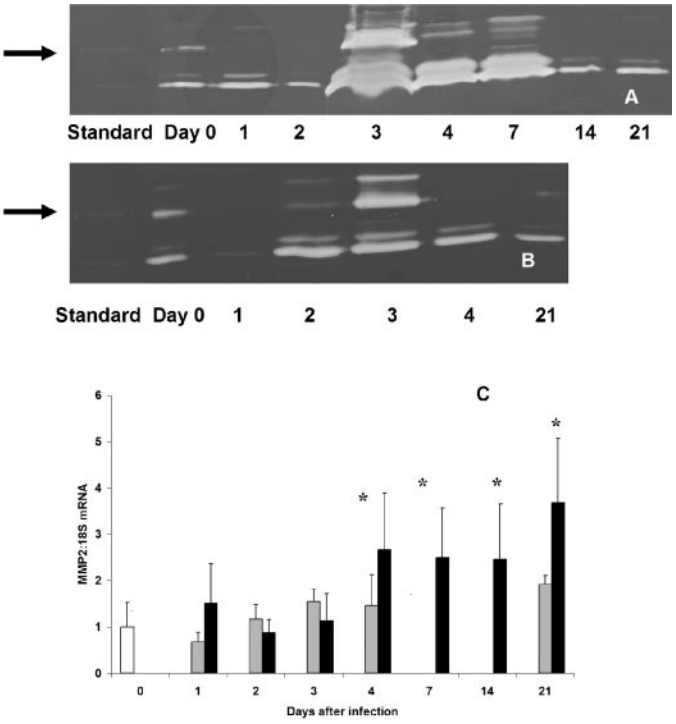

Figure 7. Matrix metalloproteinase (MMP) expression after exposure to TGF-β1. Representative zymography of peritoneal fluid for gelatinase expression. Peritoneal effluent of AdTGF-β1–treated animals (A) and the AdDL-treated animals (B) were separated on a 12% SDS-PAGE gel with gelatin. MMP-2 is the upper band in the standard lane (arrow), and MMP-9 is the lower. The zymogram identifies both pro-enzyme (upper band of couplet) and active enzyme (lower band). In all animals, there was a transient increase in MMP-2 and MMP-9 on day 3 that corresponds to peak of inflammation related to the adenovirus. AdTGF-β1 induced a sustained increase in MMP-2 and MMP-9 expression and activation in the peritoneal dialysis fluid. (C) MMP-2 gene expression measured in RNA extracted from the anterior abdominal wall normalized to untreated animals (□). ▨, Gene expression in animals that were treated with AdDL; ■, animals that were treated with AdTGF-β1. MMP-2 gene expression is significantly upregulated 4 d after infection and remains upregulated to day 21. *$P < 0.01$ AdTGF-β1 *versus* AdDL (days 1 to 4).

E-cadherin–expressing cells and E-cadherin gene expression (Figure 8A). E-cadherin expression in response to TGF-β1 was evaluated in primary culture mesothelial cells. In keeping with previous *in vitro* experiments (6), E-cadherin gene expression was downregulated by exposure to recombinant TGF-β1 in a dose-responsive manner (Figure 9). This was associated with a moderate increase in Snail gene expression. There was the expected fibrogenic response *in vitro* with upregulation of collagen and α-SMA gene expression.

Discussion

We have previously demonstrated that transient overexpression of TGF-β1 using adenovirus-mediated gene transfer leads to a persisting peritoneal fibrosis with associated angiogenesis and functional changes (15). Recent observations that EMT is involved in peritoneal fibrosis (8) and that mesothelial cells undergo EMT in response to TGF-β1 (7) led us to study the rat peritoneum after overexpression of TGF-β1 and evaluate for markers suggestive of EMT.

Our findings are strongly suggestive of the occurrence of EMT after AdTGF-β1 infection, and we have been able to characterize the sequence of events associated with TGF-β1–induced EMT. The presence of cytokeratin/α-SMA–positive cells in the mesothelium 4 d after infection with AdTGF-β1 is strong evidence of EMT. We cannot rule out that some of the α-SMA–positive submesothelial cells may be transformed fibroblasts or other cell types recruited locally or from the circulation. Snail mRNA was upregulated in the peritoneum early and coincident with evidence of EMT (day 2 after infection with AdTGF-β1). α-SMA and collagen gene expression increased by 2 d after infection, with histologic evidence of α-SMA–positive cells in the submesothelial tissue 3 d after infection.

The peak of activity occurred by day 7 with direct evidence of transitional cells with both epithelial and myofibroblast phenotype. There was extensive cellular proliferation, migration, structural re-organization, and loss of epithelial cell adhesion and continuity. MMP-2 was shown recently to be an essential component of EMT in renal tubular epithelial cells (21). Our experiments confirm that TGF-β1 upregulates MMP-2 mRNA expression and MMP-2 protein as measured by zymography. Associated with this increase in MMP-2 expression was evidence of destruction of basement membrane and movement of cells across this barrier. It is interesting that between days 7 and 14, myofibroblasts and epithelial cells were found intermingled in the submesothelial tissue.

By day 14, there was evidence that the period of destruction and rearrangement was resolving. Myofibroblasts were less evident by electron microscopy; however, α-SMA–positive cells persisted. The mesothelial integrity was again evident by day 21, with the creation of a new submesothelial basement membrane structure evident at day 14 after infection. This resolution coincides with a decrease in the gene expression of the fibrogenic cytokines α-SMA and collagen.

We evaluated the expression of Snail and E-cadherin, molecules previously implicated in EMT. Snail is a zinc finger regulator of gene expression that is upregulated in EMT (22) and seems to inhibit the mRNA expression of E-cadherin (23). We did observe increased expression of Snail mRNA early after TGF-β1 exposure both *in vivo* and in mesothelial cell culture. This is in agreement with the role of Snail as an early regulator of EMT. In previous work *in vitro*, it was observed that this increased expression of Snail inhibits E-cadherin mRNA expression and thus inhibits this important intercellular adhesion molecule (10). This loss of intercellular adhesion is a key step in EMT and allows for further transformation and migration of the affected epithelial cell (9). We confirmed that in cell culture, using our PCR assay methods, we did find a clear suppression of E-cadherin gene expression after exposure to TGF-β1, as has been described previously (6).

It is interesting that, *in vivo*, we observed an effect opposite to what was expected. E-cadherin protein expression was in-

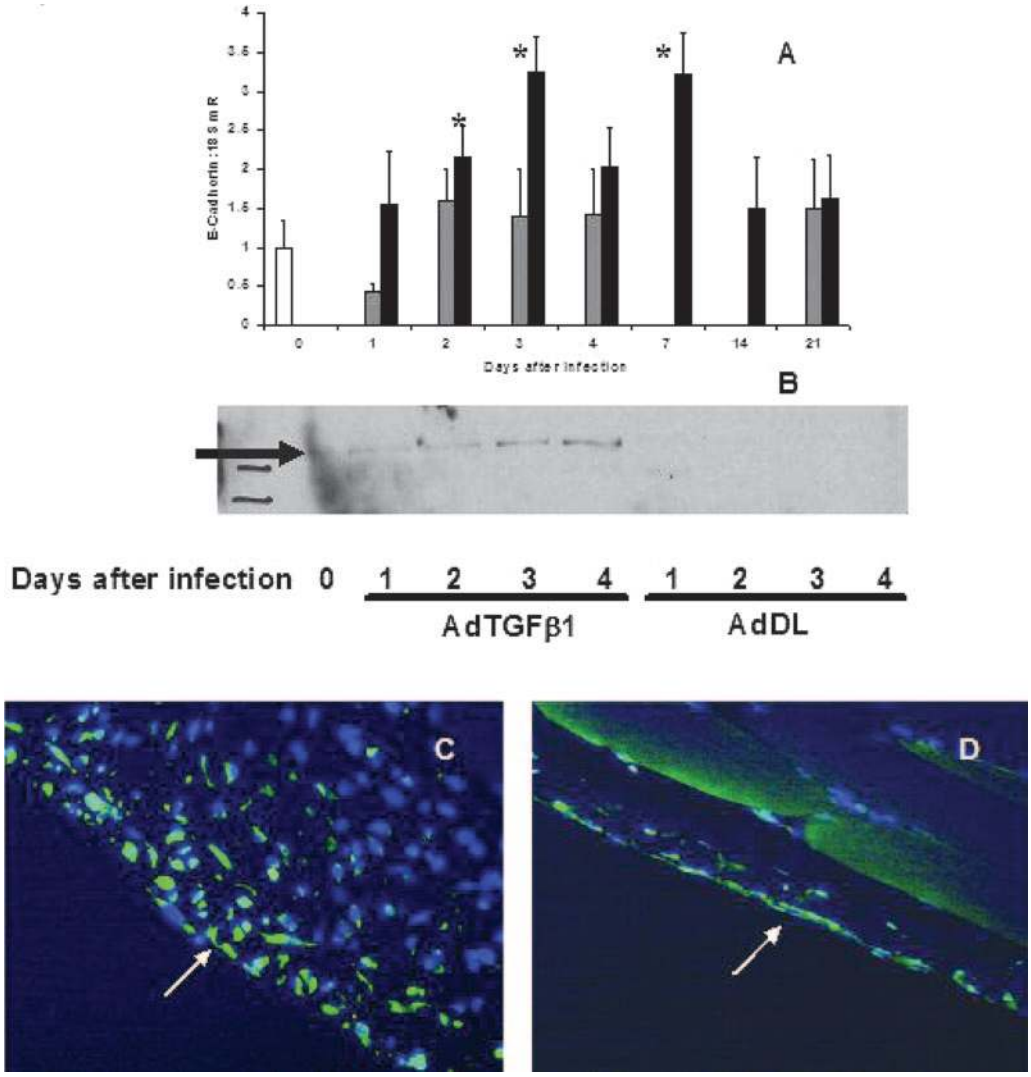

Figure 8. Peritoneal expression of E-cadherin after adenovirus infection. (A) mRNA expression in control animals (□), AdTGF-β1 (■), and AdDL (▨). (B) Protein expression in visceral peritoneal tissue analyzed by Western blot for E-cadherin (125-kD band). There was no significant increase in E-cadherin mRNA expression in AdDL-treated animals, and very low protein levels were detected. AdTGF-β1 induced a 3.5-fold increase in E-cadherin expression 3 d after infection that persisted to day 14 and was confirmed by protein expression (B). *$P < 0.001$ AdTGF-β1 *versus* control. (C and D) Parietal peritoneum sections from AdTGF-β1–treated (C) or AdDL-treated (D) animals were immunostained for E-cadherin. TGF-β1 induced an increase in cells expressing E-cadherin in the submesothelial zone (arrow). AdDL-treated animals demonstrated E-cadherin staining localized to the mesothelial cell layer (arrow). Magnification ×100.

creased after AdTGF-β1 infection, with a modest increase in E-cadherin mRNA that occurred between day 2 and day 7 with a return to baseline by day 14. This is despite histologic evidence for loss of adhesion of the mesothelial cell layer during this time. This discordance between the *in vivo* and *in vitro* regulation of E-cadherin was observed previously. Previous work in radiation induced lung fibrosis demonstrated increased immunostaining for E-cadherin in damaged lung tissue (24). We believe that the discrepancy between the *in vivo* and *in vitro* findings concerning E-cadherin likely occurs because of the effects of the local *in vivo* environment on epithelial cells. Specifically, it seems that E-cadherin–positive epithelial cells proliferate in peritoneal tissue in response to TGF-β1, increasing E-cadherin protein expression. It is also possible that TGF-β1 may positively regulate E-cadherin expression through interaction with extracellular matrix (25) and through the signaling pathway molecule SMAD4 (26), as has been described in recent publications. Clearly, this discrepant finding of E-cadherin expression warrants further investigation.

As we studied early time points after peritoneal adenovirus infection, we also evaluated peritoneal effluent and tissue for evidence of adenovirus-related inflammation. There was clearly an inflammatory response to both the control adenovirus and AdTGF-β1 that reached maximal expression 3 d after infection. This inflammatory response was no longer evident by day 4. More important, aside from a minor regulation in

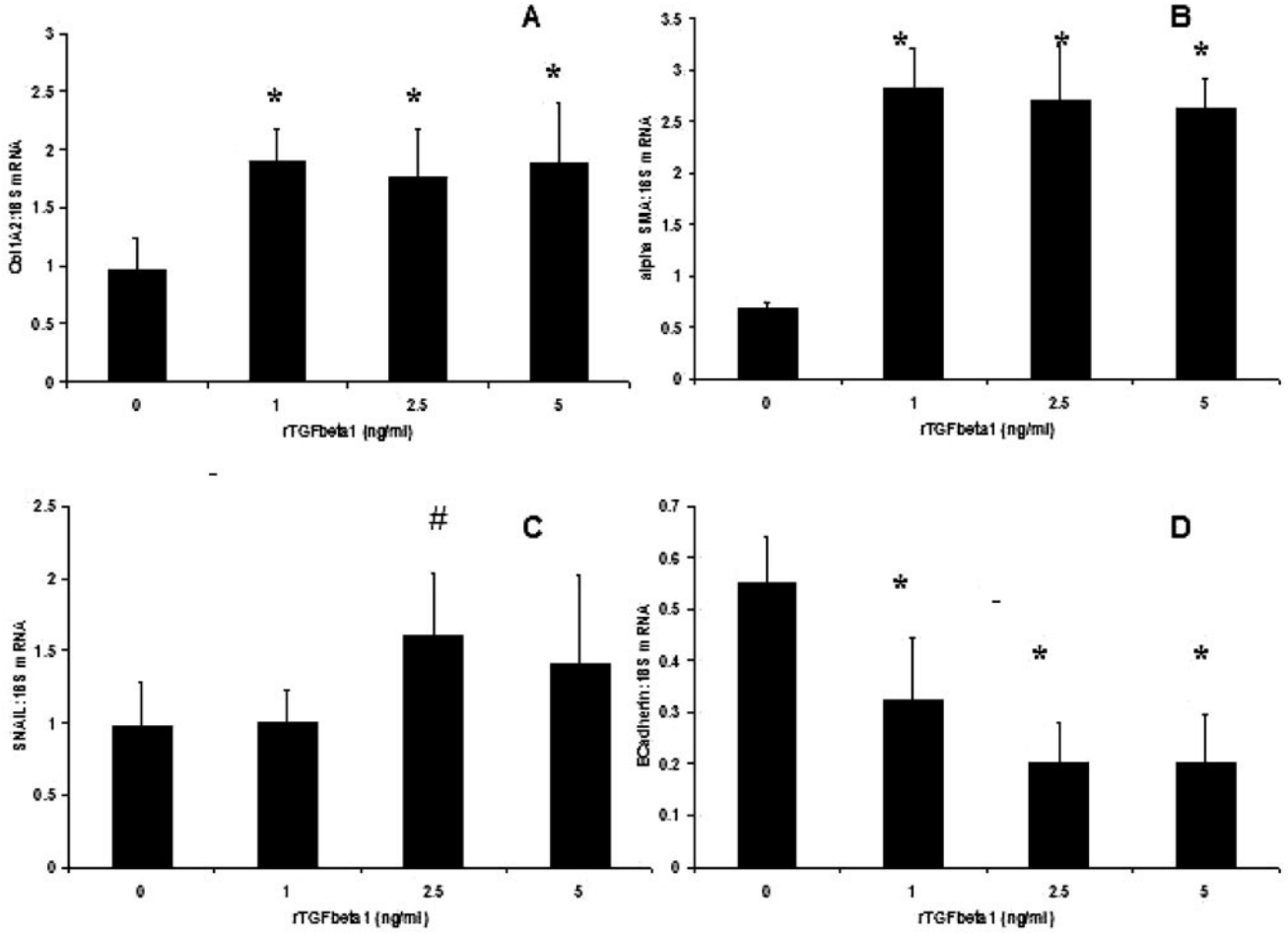

Figure 9. Response of mesothelial cells to rTGF-β1. Mesothelial cells were grown to confluence in six-well plates and exposed to 0 to 10 ng/ml of rTGF-β1 for 24 h. Cells were taken for quantitative mRNA analysis for Col1A2 (A), Snail (B), E-cadherin (C), or α-SMA (D). Results are normalized to 18S mRNA. There was the expected response of mesothelial cells to rTGF-β1 with an increased expression of Col1A2 and α-SMA (A and B). There was a suppression of E-cadherin mRNA (C) with an associated increase in Snail mRNA (D). *$P < 0.001$; #$P = 0.02$.

MMP-2 likely induced by inflammation, other markers of EMT and fibrosis were not regulated during this early inflammatory response. This indicates that TGF-β1 overexpression is responsible for the early fibrogenic changes that we observed.

In these studies, we see a general agreement between changes in mRNA expression and protein expression on the basis of immunoblot or immunohistochemistry. Specifically, there was a good temporal correlation between the immunohistochemical appearance of α-SMA–positive cells and increased mRNA expression (Figures 2 and 3). However, the correlation was not as precise between MMP-2 and E-cadherin gene and protein expression (Figures 7 and 8). This is in agreement with studies comparing genome- and proteome-wide scanning that demonstrate reasonable protein–gene correlation in large categories but poor correlation at the individual protein–gene level (27). It is interesting that this study demonstrated the poorest correlation between genes and proteins involved in cellular organization (27).

In summary, we provide further evidence that TGF-β1 induces peritoneal fibrosis, and this fibrogenesis is associated with induction of EMT. Furthermore, we have direct histologic evidence that this process occurs at an early time point and persists for at least 14 d after exposure to TGF-β1. There are few, if any, models of *in vivo* EMT. With this model, we have identified the temporal pattern of EMT and have observed discrepancies between the well studied *in vitro* and this *in vivo* response to overexpression of TGF-β1. With this model, we cannot assess other important causes of peritoneal damage seen in patients on PD, including uremia, glucose, glucose degradation products, and low pH. This model will allow for further evaluation of this important physiologic process and assessment of therapeutic intervention aimed at preventing peritoneal fibrosis.

Acknowledgments

This work was funded by Baxter Healthcare (McGaw Park, IL). P.J.M. is a CIHR Clinician Scientist. M.M.K. is a CIHR Post-Doctoral Fellow. P.B. is supported by the Bourses Lavoisier du Ministère des Affaires Etrangères, the Ligue Bourguignonne Contre le Cancer, and Bourse de voyage Boehringer.

This work was presented previously as an abstract at the American Society of Nephrology Meeting, November 14–17, 2003.

We thank Mary Jo Smith, Jessica Thoma, Cheri Bethune, Duncan Chong, and Xueya Feng for technical support.

References

1. Savagner P: Leaving the neighborhood: Molecular mechanisms involved during epithelial-mesenchymal transition. *Bioessays* 23: 912–923, 2001
2. Camenisch TD, Molin DG, Person A, Runyan RB, Gittenberger-de Groot AC, McDonald JA, Klewer SE: Temporal and distinct TGFβ ligand requirements during mouse and avian endocardial cushion morphogenesis. *Dev Biol* 248: 170–181, 2002
3. Piek E, Moustakas A, Kurisaki A, Heldin CH, ten Dijke P: TGF-(beta) type I receptor/ALK-5 and Smad proteins mediate epithelial to mesenchymal transdifferentiation in NMuMG breast epithelial cells. *J Cell Sci* 112[Suppl]: 4557–4568, 1999
4. Moustakas A, Pardali K, Gaal A, Heldin CH: Mechanisms of TGF-beta signaling in regulation of cell growth and differentiation. *Immunol Lett* 82: 85–91, 2002
5. Rastaldi MP, Ferrario F, Giardino L, Dell'Antonio G, Grillo C, Grillo P, Strutz F, Muller GA, Colasanti G, D'Amico G: Epithelial-mesenchymal transition of tubular epithelial cells in human renal biopsies. *Kidney Int* 62: 137–146, 2002
6. Fan JM, Ng YY, Hill PA, Nikolic-Paterson DJ, Mu W, Atkins RC, Lan HY: Transforming growth factor-beta regulates tubular epithelial-myofibroblast transdifferentiation in vitro. *Kidney Int* 56: 1455–1467, 1999
7. Yang AH, Chen JY, Lin JK: Myofibroblastic conversion of mesothelial cells. *Kidney Int* 63: 1530–1539, 2003
8. Yanez-Mo M, Lara-Pezzi E, Selgas R, Ramirez-Huesca M, Dominguez-Jimenez C, Jimenez-Heffernan JA, Aguilera A, Sanchez-Tomero JA, Bajo MA, Alvarez V, Castro MA, del Peso G, Cirujeda A, Gamallo C, Sanchez-Madrid F, Lopez-Cabrera M: Peritoneal dialysis and epithelial-to-mesenchymal transition of mesothelial cells. *N Engl J Med* 348: 403–413, 2003
9. Boyer B, Valles AM, Edme N: Induction and regulation of epithelial-mesenchymal transitions. *Biochem Pharmacol* 60: 1091–1099, 2000
10. Yang J, Liu Y: Dissection of key events in tubular epithelial to myofibroblast transition and its implications in renal interstitial fibrosis. *Am J Pathol* 159: 1465–1475, 2001
11. Tomasek JJ, Gabbiani G, Hinz B, Chaponnier C, Brown RA: Myofibroblasts and mechano-regulation of connective tissue remodelling. *Nat Rev Mol Cell Biol* 3: 349–363, 2002
12. Gauldie J, Sime PJ, Xing Z, Marr B, Tremblay GM: Transforming growth factor-beta gene transfer to the lung induces myofibroblast presence and pulmonary fibrosis. *Curr Top Pathol* 93: 35–45, 1999
13. Iwano M, Plieth D, Danoff TM, Xue C, Okada H, Neilson EG: Evidence that fibroblasts derive from epithelium during tissue fibrosis. *J Clin Invest* 110: 341–350, 2002
14. Williams JD, Craig KJ, Topley N, Von Ruhland C, Fallon M, Newman GR, Mackenzie RK, Williams GT, Peritoneal Biopsy Study Group: Morphologic changes in the peritoneal membrane of patients with renal disease. *J Am Soc Nephrol* 13: 470–479, 2002
15. Margetts PJ, Kolb M, Galt T, Hoff CM, Shockley TR, Gauldie J: Gene transfer of transforming growth factor-β1 to the rat peritoneum: Effects on membrane function. *J Am Soc Nephrol* 12: 2029–2039, 2001
16. Krediet RT, Lindholm B, Rippe B: Pathophysiology of peritoneal membrane failure. *Perit Dial Int* 20[Suppl 4]: S22–S42, 2000
17. Kawaguchi Y, Kawanishi H, Mujais S, Topley N, Oreopoulos DG: Encapsulating peritoneal sclerosis: Definition, etiology, diagnosis, and treatment. International Society for Peritoneal Dialysis Ad Hoc Committee on Ultrafiltration Management in Peritoneal Dialysis. *Perit Dial Int* 20[Suppl 4]: S43–S55, 2000
18. Sime PJ, Xing Z, Graham FL, Csaky KG, Gauldie J: Adenovector-mediated gene transfer of active transforming growth factor-β1 induces prolonged severe fibrosis in rat lung. *J Clin Invest* 100: 768–776, 1997
19. Bett AJ, Haddara W, Prevec L, Graham FL: An efficient and flexible system for construction of adenovirus vectors with insertions or deletions in early regions 1 and 3. *Proc Natl Acad Sci U S A* 91: 8802–8806, 1994
20. Xing Z, Ohkawara Y, Jordana M, Graham F, Gauldie J: Transfer of granulocyte-macrophage colony-stimulating factor gene to rat lung induces eosinophilia, monocytosis, and fibrotic reactions. *J Clin Invest* 97: 1102–1110, 1996
21. Cheng S, Lovett DH: Gelatinase A (MMP-2) is necessary and sufficient for renal tubular cell epithelial-mesenchymal transformation. *Am J Pathol* 162: 1937–1949, 2003
22. Carver EA, Jiang R, Lan Y, Oram KF, Gridley T: The mouse snail gene encodes a key regulator of the epithelial-mesenchymal transition. *Mol Cell Biol* 21: 8184–8188, 2001
23. Bolos V, Peinado H, Perez-Moreno MA, Fraga MF, Esteller M, Cano A: The transcription factor Slug represses E-cadherin expression and induces epithelial to mesenchymal transitions: A comparison with Snail and E47 repressors. *J Cell Sci* 116: 499–511, 2003
24. Kasper M, Huber O, Grossmann H, Rudolph B, Trankner C, Muller M: Immunocytochemical distribution of E-cadherin in normal and injured lung tissue of the rat. *Histochem Cell Biol* 104: 383–390, 1995
25. Wang H, Radjendirane V, Wary KK, Chakrabarty S: Transforming growth factor beta regulates cell-cell adhesion through extracellular matrix remodeling and activation of focal adhesion kinase in human colon carcinoma Moser cells. *Oncogene* 23: 5558–5561, 2004
26. Muller N, Reinacher-Schick A, Baldus S, van Hengel J, Berx G, Baar A, van Roy F, Schmiegel W, Schwarte-Waldhoff I: Smad4 induces the tumor suppressor E-cadherin and P-cadherin in colon carcinoma cells. *Oncogene* 21: 6049–6058, 2002
27. Greenbaum D, Jansen R, Gerstein M: Analysis of mRNA expression and protein abundance data: An approach for the comparison of the enrichment of features in the cellular population of proteins and transcripts. *Bioinformatics* 18: 585–596, 2002